

# PQ-VAE: Learning Hierarchical Discrete Representations with Progressive Quantization

Lun Huang  
Duke University  
lun.huang@duke.edu

Qiang Qiu  
Purdue University  
qqiu@purdue.edu

Guillermo Sapiro  
Duke University & Apple  
guillermo.sapiro@duke.edu

## Abstract

*Variational auto-encoders (VAEs) are widely used in generative modeling and representation learning, with applications ranging from image generation to data compression. However, conventional VAEs face challenges in balancing the tradeoff between compactness and informativeness of the learned latent codes. In this work, we propose Progressive Quantization VAE (PQ-VAE), which aims to learn a progressive sequential structure for data representation that maximizes the mutual information between the latent representations and the original data in a limited description length. The resulting representations provide a global, compact, and hierarchical understanding of the data semantics, making it suitable for high-level tasks while achieving high compression rates. The proposed model offers an effective solution for generative modeling and data compression while enabling improved performance in high-level tasks such as image understanding and generation.*

## 1. Introduction

Variational auto-encoders (VAEs) [11] are powerful tools for generative modeling and learning data efficient representations, with applications in diverse fields such as image generation, anomaly detection, and data compression. VAEs optimize the Evidence Lower Bound (ELBO) objective function that includes two terms, a reconstruction loss and a regularization term (KL divergence), encouraging the latent variables to follow a prior distribution. These two terms balance the complexity of the model and the amount of information needed to describe the input data, following the Minimum Description Length (MDL) principle [19]. The reconstruction loss and the regularization term can be seen as measures of the information in the latent code and the information required to recover the input.

We want the latent codes to be compact, meaningful, and represented by as few bits as possible. On the other hand, it is also desirable that the latent codes provide as rich infor-

mation as possible, which requires the model to be confident about the latent codes given the input. These two goals are conflicting in the ELBO. In conventional VAE objectives, a tradeoff between these two goals can be adjusted by the choice of a hyperparameter known as the beta coefficient. However, the effectiveness of this approach can depend on the particular application and choice of beta value. Furthermore, earlier works [1] have shown that a tighter ELBO does not necessarily lead to better latent representations. To address these limitations, several extensions to the VAE framework have been proposed, such as the beta-VAE [9] and total correlation (TC)-VAE [4], which aim to better balance the tradeoff between description length and information content in the latent code. However, the use of continuous latent codes in these works does not effectively reflect the description length of the codes. For example, to use them for image compression, additional steps such as scalar quantization and entropy coding are necessary, and this is not modeled as part of the original formulation.

Vector Quantized VAE (VQ-VAE) [23] is a successful discrete VAE model that uses vector quantization to discretize the continuous latent variables and achieve high compression rates, generating compact and meaningful codebooks. Its variants, such as VQ-VAE2 [18], VQ-GAN [7], and Vit-VQGAN [27], use hierarchical structures, GAN training, or transformer structures [25] to further improve reconstruction quality. However, when considering images as the data, VQ-VAE only learns small 2D tokens associated with local regions of the original image. Modeling the 2D structure can be challenging, even on a smaller scale, which requires training a heavy-weighted prior model like PixelCNN or transformers to generate images. Furthermore, since high-level tasks such as image understanding require a global understanding of the image’s semantics, VQ-VAE learns local and low-level representations that may not be suitable for such tasks.

In this work, we propose to learn a progressive sequential structure of data representations, aiming to maximize the information content in a limited (code) length. Our approach results in global, compact, and hierarchical representations,

with information organized based on its relevance to the given data. The advantages of this proposed progressive structure are manifold: 1) considerable compression rate can be achieved by encouraging the representations to be compact; 2) the representations are easier to understand, *e.g.*, for image classification, and the most important information can be easily extracted by taking the beginning part of the learned latent codes; 3) they are easier to model, for generation tasks where auto-regressive methods are prevalent, *e.g.*, image generation, the progressive structure is more natural than raster scan because the order of the latent codes inherently reflects the level of information.

Our contributions can be summarized as:

1. We propose to learn a hierarchical sequence of discrete representations.
2. We propose progressive quantization and leverage information maximization to obtain such hierarchical sequential representations.
3. Extensive experiments on image reconstruction, image generation demonstrate the superiority to other VQ-based methods.
4. Qualitative analysis shows that the learned latent codes exhibit a hierarchical structure.

## 2. Related Work

### 2.1. Representation Learning

Representation learning focuses on learning representations of data that are useful for downstream tasks. These representations are typically learned through unsupervised learning methods, which do not require explicit supervision or labels.

Classic works in representation learning include Principal Component Analysis (PCA), which finds a linear subspace that captures the most variance in the data; Independent Component Analysis (ICA), which seeks to uncover independent sources that can account for the observed data; K-means, which automatically groups data into different clusters; autoencoders, which convert data into lower-dimensional representations.

Other notable works in representation learning include Contrastive Predictive Coding (CPC) [24], which learns representations by predicting latent tokens in an auto-regressive manner; and the InfoNCE [24] objective, which learns representations by maximizing the mutual information between the input and the latent context.

Recent advances in unsupervised representation learning have focused on learning representations that capture more complex and abstract features of the data. Contrastive learning has emerged as a powerful approach for this task, where the model learns to discriminate between similar and dissimilar pairs of data points in the latent space. This approach has been used in recent works such as InfoMin [21] and SimCLR [5] to learn highly informative and transfer-

able representations that outperform previous state-of-the-art methods on various downstream tasks. Another line of recent state-of-the-art methods are masked modeling. BERT [6], GPT [15], and their variants [2, 13, 16] are successful pre-training methods in NLP. They mask out some portion of the input text and use the rest to reconstruct the missing words. MAE [8] extended this method to image data and showed success in image pre-training.

### 2.2. Variational Autoencoders

Variational autoencoders (VAEs) have become a popular approach for unsupervised representation learning. Various methods have been proposed to improve the original VAEs, including Importance Weighted Autoencoder (IWAE) [3] which uses importance sampling to improve the tightness of the lower bound, and VAE with Inverse Autoregressive Flow (VAE-IAF) [12] which replaces the simple Gaussian posterior approximation with a more flexible model.

Another line of research focuses on improving the disentanglement ability of VAEs. Beta-VAE [9] proposed a modification to the VAE objective function by adding a hyperparameter beta, which controls the trade-off between the reconstruction loss and the KL divergence term in the Evidence Lower Bound (ELBO) objective function. Factor-VAE [10] and beta-TC VAE [4] introduce additional terms in the loss function to encourage independence between different latent dimensions. Wasserstein Autoencoder (WAE) [22] uses a Wasserstein distance instead of KL divergence as the regularization term. InfoVAE employs information-theoretic principles to guide the learning of a more disentangled representation.

Finally, there is a growing interest in using VAEs for discrete data. Vector Quantized VAE (VQ-VAE) [23] employs discrete latent variables and a codebook to compress the input data, while VQGAN [7] applies additional GAN training to make the reconstruction more realistic to achieve higher compression rates. These methods have shown promising results in image compression and generative modeling.

The proposed method is related to recent advances in using VAEs for unsupervised representation learning. However, it differs by introducing a progressive structure of latent representations. This unique approach allows us to simultaneously minimize of description length and maximize the information content within the latent codes of VAEs. As a result, our method generates representations that are not only compact but also meaningful.

## 3. Background

### 3.1. VAE

Variational Autoencoders (VAEs) are a type of neural network used for generative modeling. The VAE consists of two main parts, an encoder and a decoder. The encoder maps

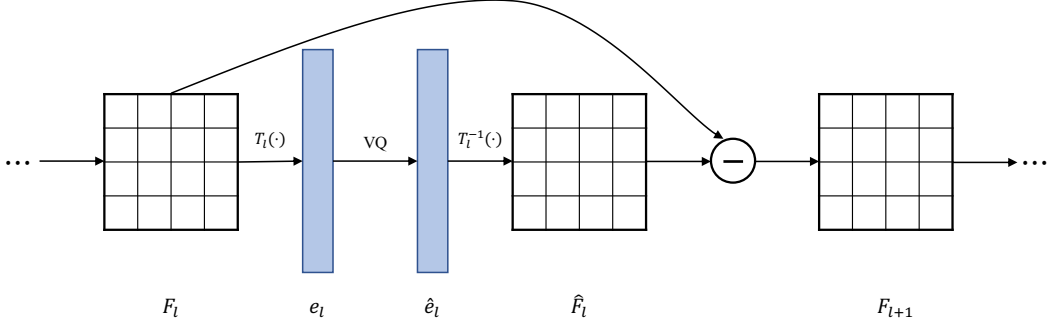


Figure 1. Overview of the progressive vector quantization. The feature map  $F_l$  at step  $l$  is converted to a feature vector  $e_l$  using a step-specific transformation  $T_l(\cdot)$ . Then  $e_l$  is quantized using a shared vector quantizer, and converted back to the reconstructed feature map  $\hat{F}_l$  with  $T_l^{-1}(\cdot)$ , the (pseudo) inverse of  $T_l$ . The subsequent feature map  $F_{l+1}$  is obtained by subtracting  $\hat{F}_l$  from  $F_l$ , with each quantization step progressively refining the representation.

the input data, such as an image, to a latent space, while the decoder maps the latent vectors back to the original data space. The encoder can be represented as a function  $q_\phi(z|x)$  modeled by parameters  $\phi$  that maps the input data  $x$  to a distribution over the latent space  $z$ . The decoder can be represented as a function  $p_\theta(x|z)$  modeled by parameters  $\theta$  that maps the latent vectors  $z$  to a distribution over the original data space  $x$ .

To train the VAE, we aim to maximize the likelihood of the observed data given the latent variable  $z$  using a variational approximation  $q(z|x)$ , which is typically chosen to be a simpler distribution such as a multivariate Gaussian. The objective function for the VAE can be written as,

$$\begin{aligned} & \log p_\theta(x) \\ & \geq \mathcal{L}(\theta, \phi) \\ & = \mathbb{E}_{q_\phi(z|x)} [\log p_\theta(x|z)] - D_{KL}(q_\phi(z|x) || p(z)), \end{aligned} \quad (1)$$

where  $\mathbb{E}$  denotes the expectation over the latent variable  $z$ , and  $D_{KL}$  is the Kullback-Leibler divergence between the variational approximation and the prior distribution  $p(z)$ . The first term in the objective function encourages the reconstructed data to be similar to the original input, while the second term regularizes the latent distribution to be close to the prior distribution.

### 3.2. VQ-VAE

Let  $x$  be the input data,  $z$  the continuous latent variable, and  $e(x)$  the encoder function that maps  $x$  to  $z$ . The vector quantization module maps the continuous latent variable  $z$  to a discrete code  $q(z)$  from the codebook  $C$ . The decoder function  $d(z)$  maps the latent variable  $z$  to the output space, such that  $d(q(z))$  approximates  $x$ . The loss function for VQ-VAE is a combination of a reconstruction loss, a codebook loss, and a commitment loss, given as,

$$\begin{aligned} \mathcal{L} = & \mathbb{E}_{x \sim p_{data}} [|x - d(q(e(x)))|^2] \\ & + \beta |\text{sg}(z) - q(z)|^2 + \gamma |z - \text{sg}(q(z))|^2, \end{aligned} \quad (2)$$

where  $x_q$  is the reconstruction of  $x$  using the code  $q(z_e)$  and  $\beta$  and  $\gamma$  are hyperparameters that control the weighting of the codebook loss and the commitment loss, respectively, and  $\text{sg}(\cdot)$  denotes the “stop gradient” operation.

The codebook loss term encourages the discrete codes to represent the input data well, and the commitment loss term encourages the encoder to commit to a code in the codebook for each input. The use of discrete codes enables VQ-VAE to learn compact and meaningful representations of the input data.

---

#### Algorithm 1 Progressive Quantization

---

```

1: Input:  $F$  : Feature map.
2: Output:  $\hat{F}$  : Quantized feature map.
3:  $z_{1:L}$  : Indexes of selected codes from the codebook.
4: Parameters: Vector quantizer (VQ); step-specific transformations  $T_{1:L}$ .
5: Initialization: Set initial feature map  $F_l = F$ .
6: procedure PROGRESSIVE QUANTIZER
7:   for  $l \leftarrow 1$  to  $L$  do
8:      $e_l = T_l(F_l)$ 
9:      $\hat{e}_l, z_l = \text{VQ}(e_l)$ 
10:     $\hat{F}_l = T_l^{-1}(\hat{e}_l)$ 
11:     $F_{l+1} = F_l - \hat{F}_l$ 
12:   end for
13:    $\hat{F} = \sum_{l=1}^L \hat{F}_l$ 
14:   return  $\hat{F}$  and  $z_{1:L}$ 
15: end procedure

```

---

### 4. Proposed Approach

We use the standard VAE encoder and decoder, but we obtain from the latent codes to be a sequential structure ordered

by their relevance to the data. Our goal is to maximize the informativeness of limited latent codes. On the one hand, the reconstruction loss in the ELBO objective reflects the information attained from the input; on the other hand, we can also measure the mutual information between the data and the latent codes, which is

$$I_q(x, z) = H(q(z)) - \mathbb{E}_{x \sim p_{data}(x)} H(q(z|x)), \quad (3)$$

*i.e.*, the entropy of the latent code distribution minus the conditional entropy given the input data. Next we will present in detail in Section 4.1 our formulation of a new training loss that maximizes information in limited discrete codes. In Section 4.2, we will further show that, guided by the proposed training objective, a meticulously designed progressive vector quantization procedure introduces a hierarchical sequential structure into representations.

#### 4.1. Maximum Information in limited discrete codes

We assume the unobserved random variable  $z$  for generating data point  $x$  is a sequence of  $L$  discrete tokens, meaning  $z \in \{(z_1, z_2, \dots, z_L) \mid z_1, z_2, \dots, z_l \in \{1, 2, \dots, K\}\}$ , where  $K$  denotes the size of the vocabulary. The sequence  $\{z_1, z_{1:2}, \dots, z_{1:L}\}$  inherently exhibits a hierarchical structure, as each subsequent term must incorporate its preceding term at the forefront of its representation. In addition, we assume the tokens are drawn independently from a uniform distribution,  $P(z_1, z_2, \dots, z_L) = \prod_{n=1, \dots, L} P(z_n) = \frac{1}{K^L}$ . Thus,

$$\text{KL}(q(z|x) \| p(z)) = L \log K - \sum_{l=1}^L H(q(z_l|x, z_{<l})). \quad (4)$$

The KL divergence between the posterior and the prior distribution, which reflects the rate needed to describe the latent code, is negatively related to the entropy of the posterior distribution. It is typically included in the conventional continuous VAE training objective so that the required number of bits is not infinity because the KL divergence between two continuous distributions is not upper-bounded. However, in the discrete settings, the KL is upper bounded. The upper bound is achieved when the conditional entropy of  $z_l$  is zero at all positions, meaning the model is absolutely confident about the choice of the latent code given the input. This is desired for meaningful representations. When the conditional entropy becomes all zero, then the KL divergence achieves its upper bound and is constant. Therefore, we remove it from the training objective.

We want to constrain that the entropy of the approximate posterior is zero. Besides, we also need to constrain that the aggregated posterior distribution matches the prior, *i.e.*,  $\text{KL}(q(z_{1:L}) \| p(z_{1:L})) = H(p(z)) - H(q(z)) = 0$ . Therefore, we add a regularization term, the negative mutual information between the data and the latent codes, to the training

loss. Finally, the proposed training loss becomes,

$$\begin{aligned} \mathcal{L} = & (\mathbb{E}_{z \sim \hat{q}(z_{1:L}|x)} \log p(x|z)) \\ & + \lambda_h \sum_{l=1}^L (H(q(z_l|x, z_{<l})) - H(q(z_l|z_{<l}))). \end{aligned} \quad (5)$$

It is non-trivial to estimate the aggregated posterior distribution  $q(z)$  as it requires enumerating the whole dataset. Even if the estimation is accurate enough, when  $H(q(z|x))$  is minimized for each  $x$  in the dataset,  $H(q(z))$  will not exceed  $\log N$ , where  $N$  is the size of the dataset. We notice that in some works  $H(q(z_l|x)) - H(q(z))$  can be further decomposed as a total correlation (TC) term plus a dimension wise KL term, and emphasize the TC term. Here we care about compactness over independence. In fact, if  $H(q(z_l|l))$  is maximized for some  $l$ , then it means that  $q(z_l) = p(z_l)$  and both the TC term and the dimension wise KL will be minimized. Therefore, we will optimize the expected entropy solely. Therefore, we relax the formulation of  $H(q(z_l|x, z_{<l})) \approx H(q(z_l|x))$ , which can be estimated easily using Monte Carlo sampling within a minibatch.

#### 4.2. Progressive Quantization

Standard VAEs convert the encoder’s feature map of the input image to a feature vector, whereas VQ-VAEs quantize each feature vector. In our approach, we convert the feature map to a feature vector and quantize it progressively, while allowing for flexibility in the size of the latent codes. Figure 1 illustrates the proposed method.

The feature map  $F$  is subjected to a sequence of quantization steps, each entailing a unique, step-specific transformation. These transformations are composed of two single-layer linear networks, acting on the spatial and channel dimensions respectively. A transformed feature  $e_l$  at step  $l$  is derived and flattened using the transformation  $T_l$ . Distances between  $e_l$  and the codebook entries are then computed, with the Gumbel-Softmax technique being utilized to sample the codebook entries. Following this, the reversed transformation of  $T_l$  is applied, utilizing the pseudo-inverse of the weight matrices, and the resultant map is subtracted from the quantized feature map. This procedure is reiterated until the predetermined maximum number of quantization steps ( $L$ ) is attained. Algorithm 1 shows the process.

#### 4.3. Feature Map Partitioning

The progressive quantization process provides a structured and precise approach to feature map quantization by utilizing step-specific reversible transformations. These transformations enhance the fidelity of the quantized feature maps. However, in the context of high-resolution images that necessitate a considerable number of latent codes—and consequently, quantization steps—the efficiency of encoding can

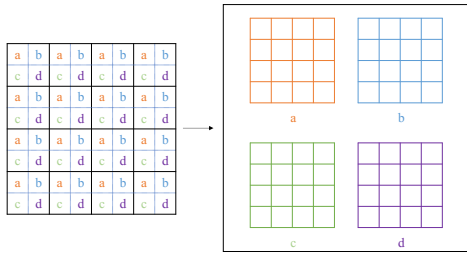


Figure 2. Example of a feature map of shape  $(1, 8, 8)$  being partitioned into  $2 \times 2$  sub-maps of shape  $(1, 4, 4)$ .

be adversely affected. Furthermore, high-resolution images are associated with large feature maps, which in turn demand an extensive number of parameters for the step-specific transformations.

To address these challenges and extend the applicability of progressive quantization to high-resolution images, we propose partitioning the feature map into a series of smaller sub-maps. These sub-maps can then be quantized progressively and in parallel, thereby improving both efficiency and parameter manageability.

Given an input feature map characterized by the shape  $(c, H, W)$ , it is initially partitioned into  $h \times w$  non-overlapping patches, each delineated by the shape  $(H/h, W/w)$  (we assume  $H, W$  can be divided even by  $h, w$  for simplicity).

Following the partitioning, feature vectors are grouped based on their relative positions within each respective patch, yielding  $\frac{H \times W}{h \times w}$  small feature maps of shape  $(c, h, w)$ . This grouping scheme ensures that each obtained code possesses an equally nearly full-size receptive field, thereby encapsulating a comprehensive, global overview of the original feature map. Figure 2 shows an example of partitioning for a feature map of shape  $(1, 8, 8)$ .

## 5. Experiments

We perform empirical evaluations of the proposed method using the MNIST, CIFAR-10 [14], CelebA and LSUN Church datasets. We measure the rate-distortion to assess its compression ability. Qualitative experimental results are also presented to investigate the generation process and illustrate the model’s ability to learn a hierarchical structure of latent representations.

### 5.1. Implementation details

For VQ-VAE, SQ-VAE and VQ-WAE, we follow the description in [20] and [26] to build models for all datasets except LSUN Church which is not included in their paper and we use the same model as in CelebA. The training details are also identical as in their settings.

For PQ-VAE, we adopt the encoder and decoder structures from dVAE [17] and use 3 ResNet blocks both for the encoder and the decoder. We transform the encoded feature to 512-dimensional. For the progressive quantization, we always partition the feature map into  $8 \times 8$  patches, and use a weight matrix of size  $64 \times 16$  to transform the spatial dimension and a weight matrix of size  $512 \times 4$  to transform the channel dimension of the feature map.

We use an initial learning rate of  $1e-3$  which is anneal at training step  $ts$  by  $e^{-\frac{ts}{25000}}$ . We use batch size 128 for MNIST, CIFAR; 512 for CelebA; and 128 for LSUN Church.

### 5.2. Reconstruction

We show the test images from MNIST, CelebA and LSUN Church and the reconstructed images from our PQ-VAE model in Table 1. For comparison, various other models including VQ-VAE, SQ-VAE [20], VQ-WAE [26] are also listed. For all methods, we use the same number of latent codes and codebooks of the same size. Specifically, the codebook size is set to 256 for MNIST and 256 for other datasets; the number of latent codes are 64 for MNIST and CIFAR10, 256 for CelebA, and 1024 for LSUN Church. For VQ-VAE, SQ-VAE, VQ-WAE, MNIST images are resized to 32x32 compressed to 8x8; CelebA images are performed a 140x140 centercrop, resized to 64x64 and then compressed to 16x16; LSUN Church images are resized to 128x128 and compressed to 32x32. For PQ-VAE, we use 64, 256 and 1024 latent codes for the three datasets respectively. The number of latent codes of PQ-VAE are not necessarily equal to the feature map size but is selected so for fair comparisons.

For quantitative assessments, we report in Table 2 the mean square error (MSE) and the reconstruction Fréchet Inception Distance (rFID) between the test images and the reconstructed images from different models. VQ-WAE is not included for comparison on CelebA and LSUN as it took too much time to train. As we can see, SQ-VAE and VQ-WAE outperforms the original VQ-VAE by a large margin in terms of both MSE and rFID. These two methods and many recent VQ-VAE based methods improve the VQ-VAE method by addressing the codebook collapse issue, which is when the codebook usage is low, thus making the training sub-optimal. Our method diverges from this kind of improvement, and improves VQ-VAE from a different perspective through the establishment of hierarchical latent codes with progressive quantization. Even so, our method shows superior performances to SQ-VAE and VQ-WAE.

### 5.3. Generation

Like all other VQ-VAE methods, to generate images, we need to learn an additional prior network to model the distribution of the latent codes. It is noteworthy that our method does not require much specific prior knowledge about model architecture of the prior network. This is because PQ-VAE

Table 1. Source images from MNIST, CelebA and LSUN Church datasets and reconstructions with different models. All models use the same number of discrete latent codes for each dataset.

Methods	MNIST	CelebA	LSUN Church
Source			
VQ-VAE			
SQ-VAE			
VQ-WAE		-	-
PQ-VAE			

Table 2. Mean Square Error (MSE) ( $\times 10^3$ ) and reconstruction Frechlet Inception Distance (rFID) of models on MNIST, CIFAR10, CelebA and LSUN Church datasets.

Methods	MNIST		CIFAR10		CelebA		LSUN Church	
	MSE	rFID	MSE	rFID	MSE	rFID	MSE	rFID
VQ-VAE	0.78	3.32	3.63	77.30	1.32	19.4	1.84	73.53
SQ-VAE	<b>0.42</b>	2.73	3.27	55.40	0.96	14.8	1.79	70.26
VQ-WAE	0.51	1.67	3.43	<b>54.30</b>	1.05	<b>14.2</b>	-	-
PQ-VAE	0.48	<b>1.51</b>	<b>2.96</b>	65.06	<b>0.82</b>	22.78	<b>1.49</b>	<b>69.98</b>

produces codes that has a hierarchy. And the latent codes in other methods presents a 2-dimensional spatial structure. Thus, CNN like models are needed for them such as Pixel-CNN, PixelSNAIL. In contrast, the latent codes of PQ-VAE is a 1-dimensional sequence and is ordered by the amount of information they possess. We can utilize sequence models for learning prior distributions. Specifically, we use a transformer to model the conditional probability of latter codes given earlier codes. For training the transformer network, apart from adding a position-specific embedding to the input, we also apply a position-specific linear transformation, which corresponds to the progressive quantization process.

We perform image generation of our method and the baseline SQ-VAE method CelebA. We visulize the generated images in Figure 3. PQ-VAE generates much shaper images than others. Looking into the details of the generated images of CelebA, we can find that face images generated by PQ-VAE are more cohesive, while images generated by other methods can have misaligned eyes, noses, mouths and etc.

#### 5.4. Studying the learned latent codes

We conduct qualitative experiments to study the learned structure of the latent codes and their importance in image reconstruction and classification.

#### 5.4.1 Representation Learning and Image Classification

We tested the representation power of PQ-VAE by applying its latent codes to image classification without additional training. We counted the occurrences of latent codes for different classes on the training set and estimated the probability of a test image belonging to a specific class using the Bayesian rule.

The estimation of a test image’s class probability is performed using two methods: “1-step conditional” and “independent” which assume that the latent codes are only dependent on a previous code or are completely independent, respectively. Please refer to Appendix for more information.

On the MNIST dataset, PQ-VAE achieves an accuracy of over 93 percent. Interestingly, for the “independent” estimation method, adding more latent codes does not always improve accuracy. This can be attributed to the learned hierarchical structure of the latent codes, where the semantic information that associates with the image class lies only in the earlier part of the latent representation, and the later part can introduce irrelevant information. Therefore, adding more latent codes beyond a certain point can lead to a decrease in accuracy.

#### 5.4.2 Measuring the amount of information in latent codes

To measure the information in a latent code, we can calculate the mutual information between the code and the input. The mutual information is not directly accessible but can be estimated in two ways by using its definition:  $I(x; z) = H(x) - H(x|z) = H(z) - H(z|x)$ . Firstly, we evaluated the importance of the latent codes at different positions by removing a latent code at a position and measuring the reconstruction MSE. Secondly, we compute the conditional entropy of a latent code given the source image and



(a) SQ-VAE



(b) PQ-VAE

Figure 3. Generated samples of SQ-VAE and PQ-VAE on CelebA.

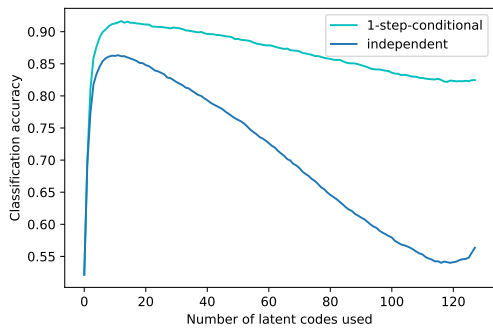
the previous codes. Figure 5 shows the results. It illustrates that removing a latent code at an early position results in a significantly larger MSE, while removing a later one does not make a big difference. This suggests that the latent codes are ordered by their importance for reconstructions, and a semantic hierarchical structure of latent codes is successfully learned. On the other hand, the conditional entropy tends to be growing as the progressive quantization goes, which also shows the amount of information is more at earlier positions. This also means the model is more confident at the beginning while more stochastic as it goes. The intuition is that semantic information, which is stored at the earlier part is more unique for a given image while the details (in the later part) are more random.

Table 3. Progressive reconstructions of the PQ-VAE model on MNIST and CelebA datasets. First  $l$  latent codes are extracted from PQ-VAE model and the rest codes are sampled from the prior network given the first  $l$  ones. The combined codes are decoded to reconstruct the source images.

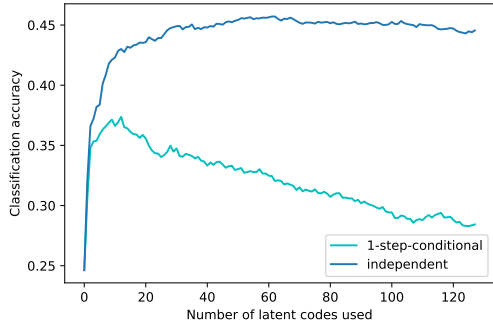
	MNIST	CelebA
Source		Source
$l=1$		$l=1$
$l=2$		$l=4$
$l=4$		$l=16$
$l=8$		$l=32$
$l=16$		$l=64$
$l=32$		$l=128$
$l=48$		$l=192$

#### 5.4.3 Progressive reconstructions

To understand what information the latent codes are possessing. We show the progressive image reconstructions of PQ-VAE in Table 3. We take the first  $l$  latent codes according to the posterior distribution of the latent codes given the source images and randomly samples the rest according to the prior distribution learned from the prior network. As it shows, even at the beginning of the process when the length is small, PQ-VAE can generate sharp images, and the reconstructions are semantically similar to the original images. At the beginning, PQ-VAE can be confused between several digit pairs. As it uses more latent codes, it becomes more confident about the semantic information, and



(a) MNIST



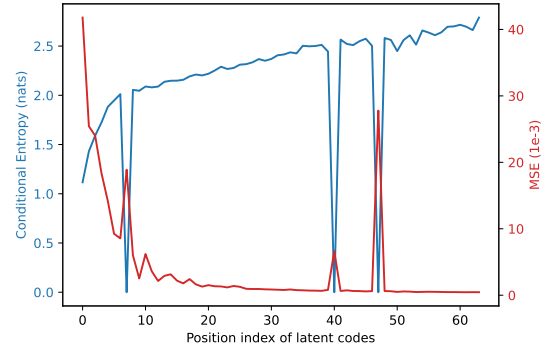
(b) CIFAR10

Figure 4. Empirical studies on classification accuracy as a function of the number of latent codes we use. On both the MNIST and the CIFAR 10 datasets, adding more latent codes will increase the accuracy when using the “1-step conditional” estimating method and then it will converge. However, for the “independent” estimating method, the accuracy will first increase and then decrease.

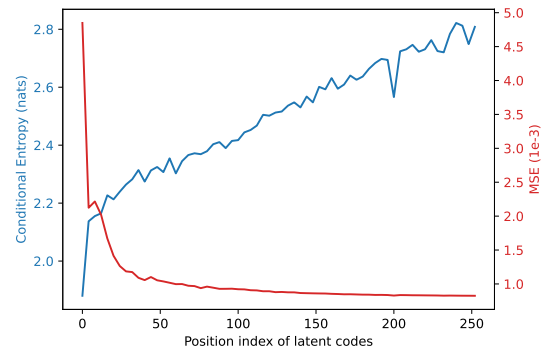
the label information is stable (from  $l=2$  for MNIST). As the length of codes keeps increasing, fine details are added to the reconstruction.

## 6. Conclusion

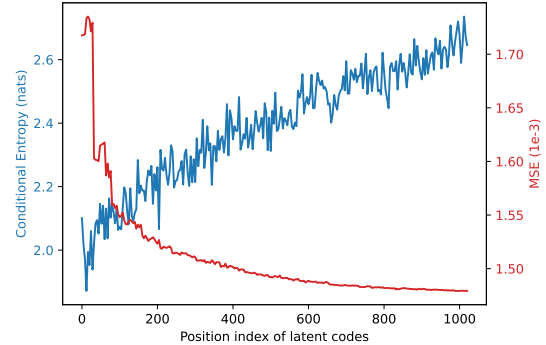
Redundancy is a common feature in data, leading to increased processing costs and difficulties in interpretation. A compact and semantic representation of the data is generally considered to be more meaningful. While traditional compression methods rely on prior knowledge of the data, recent learning methods aim to model data distributions. In this work, we propose PQ-VAE that directly maximizes information given limited data description lengths in a semantic hierarchical fashion. Our extensive empirical results demonstrate that our approach achieves superior compression rates and captures semantic information of data.



(a) MNIST



(b) CelebA



(c) LSUN Church

Figure 5. Studies of the amount of information contained in latent codes at different positions. We plot MSE as a function of removed latent code index, and the conditional entropy of a latent code given the input image and the previous codes. This graph illustrates the hierarchical significance of latent codes at different positions, indicating that earlier latent codes carry more important information compared to the later ones.

## Acknowledgments

Work partially supported by NSF, ONR, and Apple.

## References

[1] Alexander Alemi, Ben Poole, Ian Fischer, Joshua Dillon, Rif A Saurous, and Kevin Murphy. Fixing a broken elbow. In *International Conference on Machine Learning*, pages 159–168. PMLR, 2018. 1

[2] Tom Brown, Benjamin Mann, Nick Ryder, Melanie Subbiah, Jared D Kaplan, Prafulla Dhariwal, Arvind Neelakantan, Pranav Shyam, Girish Sastry, Amanda Askell, et al. Language models are few-shot learners. *Advances in neural information processing systems*, 33:1877–1901, 2020. 2

[3] Yuri Burda, Roger Grosse, and Ruslan Salakhutdinov. Importance weighted autoencoders. *arXiv preprint arXiv:1509.00519*, 2015. 2

[4] Ricky TQ Chen, Xuechen Li, Roger B Grosse, and David K Duvenaud. Isolating sources of disentanglement in variational autoencoders. *Advances in neural information processing systems*, 31, 2018. 1, 2

[5] Ting Chen, Simon Kornblith, Mohammad Norouzi, and Geoffrey Hinton. A simple framework for contrastive learning of visual representations. In *International Conference on Machine Learning*, pages 1597–1607. PMLR, 2020. 2

[6] Jacob Devlin, Ming-Wei Chang, Kenton Lee, and Kristina Toutanova. Bert: Pre-training of deep bidirectional transformers for language understanding. *arXiv preprint arXiv:1810.04805*, 2018. 2

[7] Patrick Esser, Robin Rombach, and Bjorn Ommer. Taming transformers for high-resolution image synthesis. In *Proceedings of the IEEE/CVF Conference on Computer Vision and Pattern Recognition*, pages 12873–12883, 2021. 1, 2

[8] Kaiming He, Xinlei Chen, Saining Xie, Yanghao Li, Piotr Dollár, and Ross Girshick. Masked autoencoders are scalable vision learners. In *Proceedings of the IEEE/CVF conference on computer vision and pattern recognition*, pages 16000–16009, 2022. 2

[9] Irina Higgins, Loic Matthey, Arka Pal, Christopher Burgess, Xavier Glorot, Matthew Botvinick, Shakir Mohamed, and Alexander Lerchner. beta-vae: Learning basic visual concepts with a constrained variational framework. In *International conference on learning representations*, 2016. 1, 2

[10] Hyunjik Kim and Andriy Mnih. Disentangling by factorising. In *International Conference on Machine Learning*, pages 2649–2658. PMLR, 2018. 2

[11] Diederik P Kingma and Max Welling. Auto-encoding variational bayes. *arXiv preprint arXiv:1312.6114*, 2013. 1

[12] Durk P Kingma, Tim Salimans, Rafal Jozefowicz, Xi Chen, Ilya Sutskever, and Max Welling. Improved variational inference with inverse autoregressive flow. *Advances in neural information processing systems*, 29, 2016. 2

[13] Yinhan Liu, Myle Ott, Naman Goyal, Jingfei Du, Mandar Joshi, Danqi Chen, Omer Levy, Mike Lewis, Luke Zettlemoyer, and Veselin Stoyanov. Roberta: A robustly optimized bert pretraining approach. *arXiv preprint arXiv:1907.11692*, 2019. 2

[14] Ziwei Liu, Ping Luo, Xiaogang Wang, and Xiaou Tang. Large-scale celebfaces attributes (celeba) dataset. *Retrieved August, 15(2018):11*, 2018. 5

[15] Alec Radford, Karthik Narasimhan, Tim Salimans, Ilya Sutskever, et al. Improving language understanding by generative pre-training. 2018. 2

[16] Alec Radford, Jeffrey Wu, Rewon Child, David Luan, Dario Amodei, Ilya Sutskever, et al. Language models are unsupervised multitask learners. *OpenAI blog*, 1(8):9, 2019. 2

[17] Aditya Ramesh, Mikhail Pavlov, Gabriel Goh, Scott Gray, Chelsea Voss, Alec Radford, Mark Chen, and Ilya Sutskever. Zero-shot text-to-image generation. In *International Conference on Machine Learning*, pages 8821–8831. PMLR, 2021. 5

[18] Ali Razavi, Aaron Van den Oord, and Oriol Vinyals. Generating diverse high-fidelity images with vq-vae-2. *Advances in neural information processing systems*, 32, 2019. 1

[19] Jorma Rissanen. Modeling by shortest data description. *Automatica*, 14(5):465–471, 1978. 1

[20] Yuhta Takida, Takashi Shibuya, Weihsiang Liao, Chieh-Hsin Lai, Junki Ohmura, Toshimitsu Uesaka, Naoki Murata, Shusuke Takahashi, Toshiyuki Kumakura, and Yuki Mitsufuji. Sq-vae: Variational bayes on discrete representation with self-annealed stochastic quantization. In *International Conference on Machine Learning*, pages 20987–21012. PMLR, 2022. 5

[21] Yonglong Tian, Chen Sun, Ben Poole, Dilip Krishnan, Cordelia Schmid, and Phillip Isola. What makes for good views for contrastive learning? *Advances in neural information processing systems*, 33:6827–6839, 2020. 2

[22] Ilya Tolstikhin, Olivier Bousquet, Sylvain Gelly, and Bernhard Schoelkopf. Wasserstein auto-encoders. *arXiv preprint arXiv:1711.01558*, 2017. 2

[23] Aaron Van Den Oord, Oriol Vinyals, et al. Neural discrete representation learning. *Advances in neural information processing systems*, 30, 2017. 1, 2

[24] Aaron Van den Oord, Yazhe Li, and Oriol Vinyals. Representation learning with contrastive predictive coding. *arXiv e-prints*, page arXiv: 1807.03748, 2018. 2

[25] Ashish Vaswani, Noam Shazeer, Niki Parmar, Jakob Uszkoreit, Llion Jones, Aidan N Gomez, Łukasz Kaiser, and Illia Polosukhin. Attention is all you need. In *Advances in neural information processing systems*, pages 5998–6008. 1

[26] Tung-Long Vuong, Trung Le, He Zhao, Chuanxia Zheng, Mehrtash Harandi, Jianfei Cai, and Dinh Phung. Vector quantized wasserstein auto-encoder. *arXiv preprint arXiv:2302.05917*, 2023. 5

[27] Jiahui Yu, Xin Li, Jing Yu Koh, Han Zhang, Ruoming Pang, James Qin, Alexander Ku, Yuanzhong Xu, Jason Baldridge, and Yonghui Wu. Vector-quantized image modeling with improved vqgan. *arXiv preprint arXiv:2110.04627*, 2021. 1